Protein Expression and Purification 68 (2009) 208–214

Contents lists available at ScienceDirect

Protein Expression and Purification

journal homepage: www.elsevier.com/locate/yprep

# *Escherichia coli* expression and *in vitro* activation of a unique ligninolytic peroxidase that has a catalytic tyrosine residue

Yuta Miki [a], María Morales [a], Francisco J. Ruiz-Dueñas [a], María Jesús Martínez [a], Hiroyuki Wariishi [b], Angel T. Martínez [a,*]

[a] Centro de Investigaciones Biológicas, CSIC, Ramiro de Maeztu 9, E-28040 Madrid, Spain
[b] Faculty of Agriculture, Kyushu University, 6-10-1 Hakozali, Higashi-ku, Fukuoka 812-8581, Japan

ARTICLE INFO

*Article history:*
Received 20 May 2009
and in revised form 1 June 2009
Available online 6 June 2009

*Keywords:*
Lignin peroxidase
*Trametes cervina*
Heme protein
*Escherichia coli* expression
*In vitro* activation
Veratryl alcohol

ABSTRACT

Heterologous expression of *Trametes cervina* lignin peroxidase (LiP), the only basidiomycete peroxidase that has a catalytic tyrosine, was investigated. The mature LiP cDNA was cloned into the pET vector and used to transform *Escherichia coli*. Recombinant LiP protein accumulated in inclusion bodies as an inactive form. Refolding conditions for its *in vitro* activation—including incorporation of heme and structural $Ca^{2+}$ ions, and formation of disulfide bridges—were optimized taking as a starting point those reported for other plant and fungal peroxidases. The absorption spectrum of the refolded enzyme was identical to that of wild LiP from *T. cervina* suggesting that it was properly folded. The enzyme was able to oxidize 1,4-dimethoxybenzene and ferrocytochrome *c* confirming its high redox potential and ability to oxidize large substrates. However, during oxidation of veratryl alcohol (VA), the physiological LiP substrate, an unexpected initial lag period was observed. Possible modification of the enzyme was investigated by incubating it with $H_2O_2$ and VA (for 30 min before dialysis). The pretreated enzyme showed normal kinetics traces for VA oxidation, without the initial lag previously observed. Steady-state kinetics of the pretreated LiP were almost the same as the recombinant enzyme before the pretreatment. Moreover, the catalytic constant ($k_{cat}$) for VA oxidation was comparable to that of wild LiP from *T. cervina*, although the Michaelis–Menten constant ($K_m$) was 8-fold higher. The present heterologous expression system provides a valuable tool to investigate structure–function relationships, and autocatalytic activation of the unique *T. cervina* LiP.



Lignin in wood and other lignocellulosic materials is the most abundant renewable aromatic polymer, and one of the most recalcitrant biomaterial on the earth [1,2]. Lignin peroxidase (LiP[1]; EC: 1.11.1.14), first described in the white-rot basidiomycete *Phanerochaete chrysosporium* [3–5], is an extracellular heme peroxidase involved in the oxidative depolymerization of lignin by white-rot fungi. Different aspects of LiP molecular structure provide to this enzymes the high redox potential and ability to oxidize bulky substrates, required for lignin biodegradation [6,7]. These unique properties of LiP have been shown by oxidation of 1,4-dimethoxybenzene [8] and ferrocytochrome *c* [9], as well as by its action on polymeric lignin and different model compounds [10,11]. 1,4-Dimethoxybenzene is hardly oxidized by other peroxidases because of its high redox potential ($E_{1/2}$ 1.34 V), and ferrocytochrome *c* is too large to penetrate into the heme cavity, as is also the case with the large lignin macromolecule. The catalytic properties of LiP and other ligninolytic enzymes are of interest for applications in paper pulp bleaching and bioethanol production from woody biomass [12].

Several kinetic, crystallographic and spectroscopic studies including chemical modification and site-directed mutagenesis of LiP from *P. chrysosporium* have demonstrated that a tryptophan residue located at the surface of the protein (Trp171) is the oxidation site for high redox-potential aromatic substrates [13–17] (Fig. 1A). This implies the existence of a long-range electron transfer (LRET) pathway from this exposed Trp171 to the heme cofactor in the peroxide activated enzyme. Studies of versatile peroxidases (VP) from *Pleurotus eryngii* and *Pleurotus ostreatus*, which possess catalytic properties of LiP including veratryl alcohol (VA) oxidation, have shown that one of the VP substrates oxidation sites is also a tryptophan residue at the same location of *P. chrysosporium* LiP Trp171 [18–20]. In fact, the tryptophan residue corresponding to the above Trp171 is conserved in all genes encoding LiP and VP

* Corresponding author. Fax: +34 915360432.
*E-mail address:* atmartinez@cib.csic.es (A.T. Martínez).

[1] *Abbreviations used:* ABTS, 2,2′-azino-bis(3-ethylbenzothiazoline-6-sulfonate); DTT, dithiothreitol; EDTA, ethylenediaminetetraacetic acid; GSH, reduced glutathione; GSSH, oxidized glutathione; HRP, horseradish peroxidase; IPTG, isopropyl-β-D-thiogalactopyranoside; $k_{cat}$, catalytic constant; $K_m$, Michaelis–Menten constant; LiP, lignin peroxidase; LiP*, recombinant LiP; p-LiP*, pretreated LiP*; LRET, long-range electron transfer; MnP, manganese peroxidase; PCR, polymerase chain reaction; SDS–PAGE, sodium dodecyl sulfate–polyacrylamide gel electrophoresis; VA, veratryl alcohol.

1046-5928/$ - see front matter © 2009 Elsevier Inc. All rights reserved.
doi:10.1016/j.pep.2009.06.003

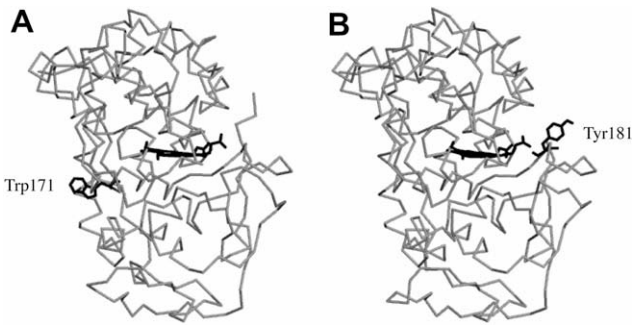


**Fig. 1.** General scheme of the *P. chrysosporium* (A) and *T. cervina* LiP (B) molecular structures showing the protein backbone, the heme cofactor (in the center), and the aromatic residues involved in catalysis being Trp171 and Tyr181, respectively. PDB entry 1LLP is shown in (A), while a theoretical structure obtained by homology modeling [27] is shown in (B). Homology modeling was performed with the Molecular Operating Environment (MOE) program (Chemical Computing Group), using 1LLP structure as template.

proteins [21,22]. Thus, this residue is considered as essential for the LiP-type catalytic mechanism including the LRET pathway from high redox-potential substrates to heme.

Recently, a novel type of LiP has been found in the white-rot basidiomycete *Trametes cervina*. *T. cervina* LiP can oxidize 1,4-dimethoxybenzene and ferrocytochrome *c* indicating that it possesses high redox potential and the ability to oxidize bulky substrates like other LiP and VP [23]. However, a tryptophan residue homologous to the catalytic tryptophan of LiP and VP is absent from the *T. cervina* LiP sequence [24]. By contrast, its sequence contains one tyrosine residue (Tyr181), while no tyrosines are present in the sequences of other LiP and VP [21]. It has been reported that tyrosine can act as a redox active residue, like tryptophan, in different enzymes [25] and a tyrosyl radical has been detected in a VP variant, whose catalytic tryptophan had been substituted by tyrosine [26].

The theoretical structure obtained by homology modeling of the *T. cervina* enzyme has shown that Tyr181 is exposed at the protein surface being a candidate substrate oxidation site (Fig. 1B), in agreement with results from chemical modification studies [27]. The catalytic mechanism of *T. cervina* LiP, most probably involving a Tyr181 radical, is quite interesting but it has not been investigated so far because of the very low yield of wild enzyme obtained from *T. cervina* cultures. Thus, developing an expression system to obtain recombinant LiP (LiP$^*$) of *T. cervina* was a requisite for further detailed mechanistic studies including site-directed mutagenesis of this unique peroxidase. In the present study, a heterologous system for *T. cervina* LiP$^*$ expression in *Escherichia coli* was constructed. Since LiP$^*$ protein was located in inclusion bodies, as other recombinant plant and fungal peroxidases expressed in *E. coli* [28–31], *in vitro* refolding was optimized for activation of *T. cervina* LiP$^*$. Finally, the physiochemical and catalytic properties of the purified LiP$^*$ were determined, and some interesting results were observed during VA oxidation.

## Materials and methods

### *Materials*

Dithiothreitol (DTT), lysozyme, oxidized glutathione (GSSG), hemin, 1,4-dimethoxybenzene, VA, and ferricytochrome *c* were purchased from Sigma–Aldrich. Isopropyl-β-D-thiogalactopyranoside (IPTG) was from Calbiochem, and 2,2′-azino-bis(3-ethylbenzothiazoline-6-sulfonate) (ABTS) and DNase I were from Boehringer Mannhein. Restriction enzymes were from New England Biolabs. All other chemicals were from Merk. *E. coli* expression vector pET23a(+) and BL21(DE3)pLysS strain were from Merck.

### *Amplification of cDNA encoding the mature T. cervina LiP*

The mature LiP sequence was deduced from multiple alignment of the *T. cervina* LiP predicted amino-acid sequence (GenBank Accession No.: AB191466) with those of *Pl. eryngii* VPL2 (AF007224) and *P. chrysosporium* LiPH8 (M27401) where the beginning of mature protein had been localized. Two oligonucleotides were synthesized corresponding to the N-terminal and C-terminal sequences of the mature *T. cervina* LiP: oligonucleotide *lip-S* (5′-CCAT **ATG** GTG AGC TGC GGT GGC GGC CGG-3′) corresponded to the first seven residues preceded by a NdeI restriction site, and oligonucleotide *lip-A* (5′-GGGA TCC **TTA** CCC GAG AAC GGG GGC AAC-3′) was reverse and complementary to the last seven codons with a BamHI restriction site following the termination codon.

The mature LiP cDNA (*mlip*) was amplified by polymerase chain reaction (PCR) with *Taq* polymerase, using the cDNA of *T. cervina* LiP gene (AB191466) as template, and the *lip-S* and *lip-A* as primers. PCR temperature and time were programmed as follows; 94 °C for 2 min, followed by 94 °C for 60 s, 58 °C for 60 s, and 72 °C for 90 s in 30 cycles, with a final 5 min extension at 72 °C. PCR products were separated electrophoretically using 1.0% agarose gel, and stained with ethidium bromide. The DNA fragment corresponding to amplified *mlip* was excised from the gel and extracted using Geneclean kit (Funakoshi). Purified *mlip* was cloned into pGEM T-easy vector (Promega). Correct DNA sequence and reading frame were confirmed by sequencing using a BigDye terminator v3.1 equipment (Applied Biosystems).

### *Vector construction and mlip expression in E. coli*

The *mlip* cDNA was excised with NdeI and BamHI from pGEM T-easy vector, and inserted under T7 promoter into the multi-cloning region of pET23a vector previously digested with the same enzymes. The resulting construct (named pET-*mlip*) was used to transform *E. coli* BL21(DE3)pLysS.

*Escherichia coli* cells harboring pET-*mlip* were grown in Terrific Broth containing ampicillin (100 μg/mL) and chloramphenicol (34 μg/mL) shaken (250 rpm) at 37 °C until an $OD_{500}$ of 1.0 was attained. The cultures were induced by addition of 1.0 mM IPTG, and cultivated for another 4 h. Bacterial pellets harvested by centrifugation were stored at −20 °C until processed as described below.

### *Extraction and solubilization of the inclusion bodies*

Fifteen grams of bacterial pellet (wet weight) were suspended in 200 mL of 50 mM Tris–HCl buffer (pH 8.0) containing 10 mM ethylenediaminetetraacetic acid (EDTA), 5 mM DTT, and 0.1 mg/mL DNase. Cells were disrupted by sonication, and subsequent centrifugation (30 min at 16,000*g*) allowed the collection of inclusion bodies containing the LiP$^*$ polypeptide. Inclusion bodies were washed twice with 20 mM Tris–HCl buffer (pH 8.0) containing 1 mM EDTA and 1 mM DTT, and solubilized in the same buffer, containing 8 M urea, at room temperature. Protein concentration was determined by the Bradford method [32] using bovine serum albumin as standard, and then adjusted to 2 mg/mL using the same urea buffer. Finally the solution was sonicated for 1 min × 3 times at 20,000 Hz frequency.

### *Optimization of the in vitro refolding of T. cervina LiP$^*$*

The refolding mixture was prepared by 10-fold dilution of the above solution with refolding solution containing urea, $CaCl_2$,

hemin, and GSSG in Tris–HCl buffer at given pH values. The refolding conditions were optimized in small-scale experiments (10 mL). Conditions remaining constant were: 50 mM Tris–HCl buffer, 0.1 mM EDTA, and 0.1 mM DTT. Parameters systematically varied included urea (0–2.0 M), GSSG (0–2.0 mM), hemin (0–40 μM), $CaCl_2$ (0–10 mM), pH (7.0–11.0), incubation time (12–72 h), and temperature (4 °C or room temperature). Refolding efficiency was estimated from ABTS oxidation in the above mixtures. The ABTS oxidation assay was carried out in 20 mM succinate buffer (pH 4.5) containing 0.5 mM ABTS and 0.1 mM $H_2O_2$. Reaction was initiated by addition of $H_2O_2$, and monitored at 420 nm (ABTS cation radical $\varepsilon_{420\,nm}$ 36 $mM^{-1}$ $cm^{-1}$). One activity unit was defined as the amount of enzyme oxidizing 1 μmol of ABTS per 1 min.

### *Large-scale refolding and LiP* purification*

The inclusion bodies were solubilized as described above, but the solubilization solution was 50 mM Tris–HCl buffer (pH 8.0) containing 2 mM EDTA and 2 mM DTT. Large-scale refolding of LiP* was performed under the optimal conditions established in the small-scale experiments. Final concentrations in the refolding mixture were: 5 mM $CaCl_2$, 0.6 mM GSSG, 0.1 mM DTT, 0.4 M urea, 5 μM hemin, and 0.1 mM EDTA in 50 mM Tris–HCl (pH 9.5). After 18 h incubation at room temperature in the dark, the mixture was 50-fold concentrated using a 3 kDa cut-off ultrafiltration membrane. The concentrated sample was first dialyzed against 20 mM sodium acetate buffer (pH 4.2) containing 5 mM $CaCl_2$, and then against 20 mM sodium acetate buffer (pH 4.5) containing 1 mM $CaCl_2$. Insoluble material was eliminated by centrifugation at 16,000*g* for 30 min. The supernatant including active LiP* was dialyzed against 10 mM sodium acetate buffer (pH 6.0) containing 1 mM $CaCl_2$. LiP* was purified in an anion-exchange chromatography column (Pharmacia Resource Q) using a 0–0.3 M NaCl gradient in the latter $CaCl_2$-containing 10 mM sodium acetate buffer (pH 6.0). Purified LiP* was dialyzed against 20 mM sodium succinate buffer (pH 4.5) containing 1 mM $CaCl_2$, and stored at −80 °C.

### *Physicochemical and catalytic properties of the refolded LiP**

Sodium dodecyl sulfate–polyacrylamide gel electrophoresis (SDS–PAGE) was performed in 12% polyacrylamide gel. Protein bands were visualized with Coomassie Blue R-250.

To investigate thermal stability, 1 μM LiP* was incubated for 30 min in 20 mM sodium succinate buffer (pH 4.5) containing 1 mM $CaCl_2$ at different temperatures, and ABTS oxidation was assayed. For pH stability assay, 1 μM LiP* was incubated for 30 min at room temperature in 20 mM sodium succinate buffer (pH 2.5–6.0) or 10 mM Tris–HCl buffer (pH 7.0–9.0) containing 1 mM $CaCl_2$, and ABTS oxidation activity was measured under the same conditions described above, using 20 mM succinate buffer (pH 3.5).

Oxidation of 1,4-dimethoxybenzene was investigated in 20 mM sodium succinate buffer (pH 3.5) containing 78 nM enzyme, 0.2 mM substrate, and 0.1 mM $H_2O_2$. Reactions were initiated by addition of $H_2O_2$. Spectral changes were monitored with a diode array UV–vis spectrophotometer (Hewlett–Packard 8453).

The oxidation of ferrocytochrome *c* was assayed as previously described [9,23]. Ferrocytochrome *c* was prepared by reducing ferricytochrome *c* with sodium dithionite. Excess sodium dithionite was removed using Sephadex G-25. The reaction mixture contained 78 nM enzyme, 12 μM substrate, and 0.1 mM $H_2O_2$ in 20 mM succinate buffer (pH 4.0).

### *VA steady-state kinetics and LiP* pretreatment with VA and $H_2O_2$*

VA oxidation rates were estimated from maximal absorbance increase at 310 nm for 5 s (veratraldehyde $\varepsilon_{310\,nm}$ 9.3 $mM^{-1}$ $cm^{-1}$) [5]. $K_m$ and catalytic constant ($k_{cat}$) were obtained by nonlinear least-squares fitting to the experimental measurements using the Michaelis–Menten model equation: $v = (k_{cat}/K_m)[S]/(1 + [S]/K_m)$.

LiP* was treated with 50 equivalents of $H_2O_2$ in 20 mM sodium succinate buffer (pH 4.5) containing 1 mM $CaCl_2$ and 10 mM VA and, after 30 min incubation at room temperature, dialyzed against the same $CaCl_2$-containing buffer.

## Results and discussion

### *Vector construction and LiP* protein production in E. coli*

The *mlip* sequence encoding the mature *T. cervina* LiP, which was deduced from multiple alignment of fungal peroxidase N-terminal sequences (Fig. 2A), was successfully amplified by PCR, and inserted into the expression vector pET23a(+) (Fig. 2B). The resulting construct pET-*mlip* was transformed into *E. coli* BL21(DE3)pLysS. After induction with IPTG, the positive transformant produced large quantities of LiP* protein (about 80 mg/L) that accumulated in insoluble inclusion bodies with approximately 80% purity (Fig. 2C).

### *In vitro refolding of LiP**

The refolding parameters were optimized in small-scale experiments (Fig. 3). Firstly, urea concentration was investigated. The optimal urea concentrations for horseradish peroxidase (HRP), *P. chrysosporium* LiP, and *P. chrysosporium* manganese peroxidase (MnP) have been determined to be 2.0 M [28–30]. Only for *Pl. eryngii* VP refolding a much lower optimal urea concentration (0.15 M) has been reported [31]. In refolding of the *T. cervina* LiP*, ABTS oxidation was detected in the range of 0.1–2.0 M urea concentration, with the maximum activity being obtained when using 0.4 M urea (Fig. 3A).

Two $Ca^{2+}$ ions, which are conserved in the general structure of all plant and fungal peroxidases, are essential for correct folding and structural stability of these enzymes [21]. In refolding of HRP, *P. chrysosporium* LiP and *Pl. eryngii* VP, 5 mM $CaCl_2$ was the optimal concentration [28,30,31], and 50 mM $CaCl_2$ was used for *P. chrysosporium* MnP refolding [31]. In refolding of *T. cervina* LiP*, the optimal concentration of $CaCl_2$ was 5 mM (Fig. 3B).

Plant and fungal peroxidases generally have 4–5 disulfide bonds, and the analysis of the primary and putative tertiary structures of *T. cervina* LiP suggested that it could also have four

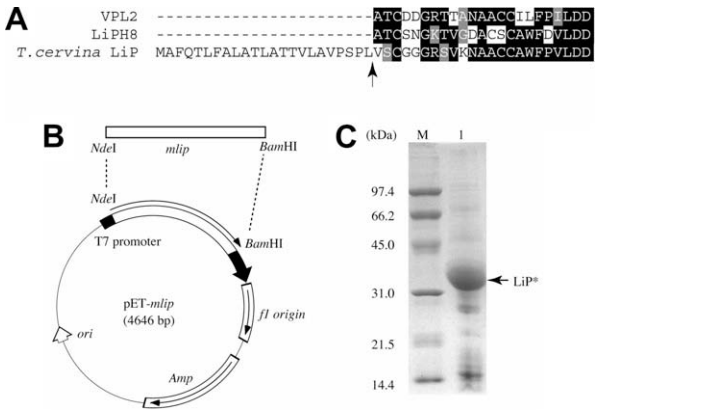


**Fig. 2.** Vector construction and *T. cervina* LiP protein production in *E. coli*. (A) Multiple alignment of N-termini sequences of mature *Pl. eryngii* VPL2 and *P. chrysosporium* LiPH8, and whole *T. cervina* LiP, for prediction of the putative signal peptide cleavage site in the latter enzyme (arrow). (B) Expression vector pET-*mlip* including the mature LiP cDNA sequence (*mlip*). (C) SDS–PAGE of inclusion bodies showing LiP* protein over-expressed in *E. coli* (lane 1). Molecular mass standards are included (lane M).

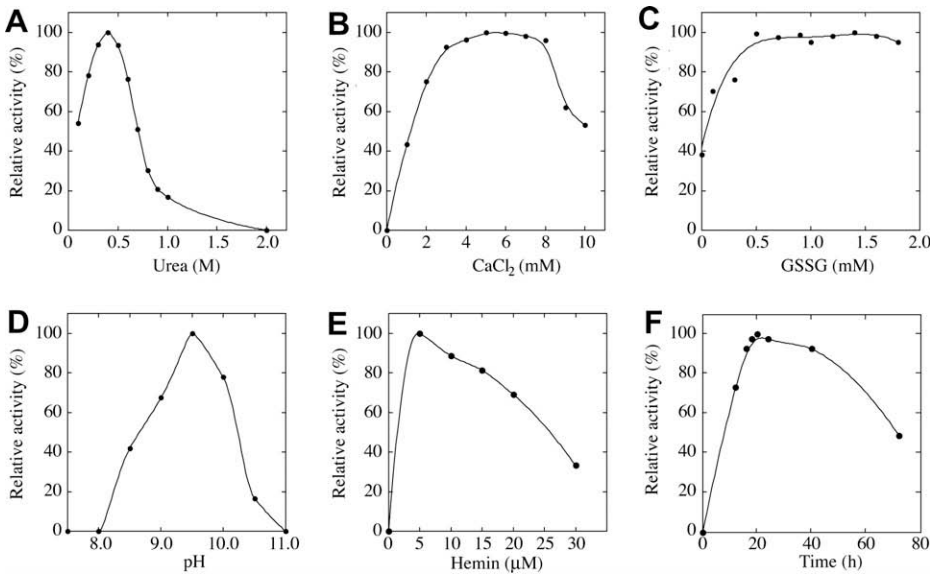


**Fig. 3.** Parameter optimization for the *in vitro* refolding of LiP*. The basic conditions were: 18 h incubation at 24 °C in 50 mM Tris–HCl buffer (pH 9.5) containing 0.4 M urea, 0.7 mM GSSG, 5 mM $CaCl_2$, 0.1 mM DTT, 0.1 mM EDTA, and 5 μM hemin. The six parameters systematically varied were: (A) urea concentration, (B) $CaCl_2$ concentration, (C) GSSG concentration, (D) pH, (E) hemin concentration, and (F) incubation time. Refolding efficiency was estimated by ABTS oxidation in small-scale refolding assays (see Materials and methods), and shown as relative activity of maximal yields.

disulfide bonds [24]. In refolding, the formation of disulfide bonds is facilitated by controlling the ratio of oxidized-to-reduced glutathione (GSSG/GSH). As shown in Fig. 3C, the LiP* activity increased in a GSSG concentration-dependent manner up to 0.6 mM, and was stable over this concentration. When using 0.6 mM GSSG (the minimum amount required for the maximal activity) together with 0.1 mM DTT, the GSSG/GSH ratio was 5:2, which is similar to those used for other plant and fungal peroxidases [28–31].

The pH of the refolding mixture influences disulfide bond formation and peroxidase stability. Optimal pH was found to be pH 8.0 for HRP and *P. chrysosporium* MnP [28,29], and pH 9.5 for *P. chrysosporium* LiP and *Pl. eryngii* VP* [30,31]. The optimum pH for refolding *T. cervina* LiP was determined to be pH 9.5 (Fig. 3D).

Finally, the optimal concentration of exogenous hemin was 5 μM (Fig. 3E), and the optimal incubation conditions were found to be 18–20 h at room temperature (Fig. 3F).

### *Purification of refolded LiP**

Large-scale (2–4 L) refolding of LiP* was carried out under the conditions optimized above. After incubation, the refolding mixture including active LiP* was concentrated and dialyzed. The dialysis step allowed elimination of additives and precipitation of the misfolded protein, yielding a supernatant with 30-fold purification factor (Table 1). Then, LiP* was purified by single-step anion-exchange chromatography using a Resource Q column (Fig. 4). The purified LiP* gave a single band on SDS–PAGE (Fig. 4, inset). The final yield calculated from total activity was 23%, and the purification factor was 60-fold. Refolding efficiency based on final specific activity was approximately 2%; and the final yield of pure LiP* against initial amount of LiP* protein in the refolding mixture was approximately 0.6%, which is the same rate reported for recombinant LiP and MnP from *P. chrysosporium* [29,30].

The absorption spectrum of LiP* with peaks at 407, 501, and 637 nm was identical to that of the wild enzyme from *T. cervina* culture, suggesting that the protein folding, heme insertion, and iron coordination were correct. The molar extinction coefficient at 407 nm was determined to be 147 $mM^{-1}\,cm^{-1}$, which is the same value of the wild enzyme.

**Table 1**
Purification of *E. coli*-expressed *T. cervina* LiP* after its *in vitro* refolding, using large-scale conditions.

| | Protein (mg) | Total activity (U) | Specific activity (U/mg) | Yield (%) | Purification (folds) |
|---|---|---|---|---|---|
| Refolding mixture | 492 | 133,000 | 270 | 100 | 1 |
| Dialysis | 5.2 | 42,000 | 8080 | 32 | 30 |
| Resource Q | 1.9 | 31,000 | 16,300 | 23 | 60 |

From 5-L culture containing approximately 15 g cells (wet weight), and 2 g of total protein from Bradford estimation after lysis.

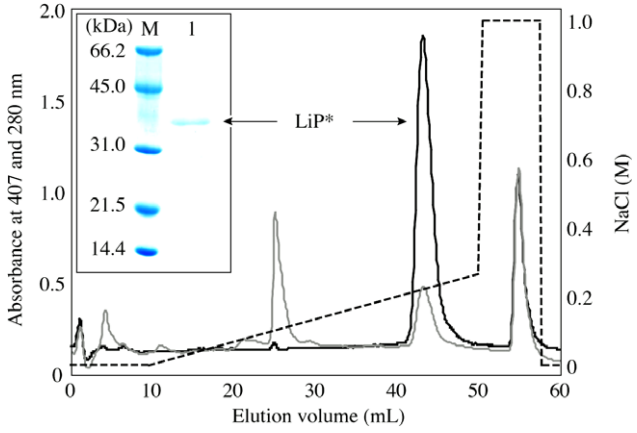


**Fig. 4.** Purification of the refolded LiP*. Resource Q elution profile, showing absorbance at 407 nm (black line) and 280 nm (gray line), and NaCl gradient (dashed line). The inset shows SDS–PAGE of pure LiP* from the arrowed peak (lane 1) and molecular mass standards (lane M).

### *LiP* stability and catalytic properties*

Thermal and pH stabilities of *T. cervina* LiP* were investigated. The recombinant enzyme was fully stable up to 30 °C but unstable

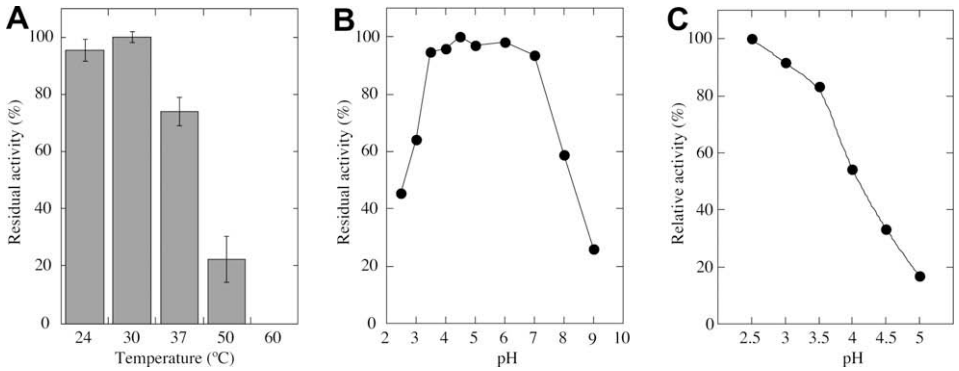


**Fig. 5.** LiP* stability and pH dependence, estimated for VA oxidation. (A) Thermal stability showing residual activities after 30 min incubation at the given temperatures. (B) pH stability showing residual activities after 30 min incubation at 24 °C in different pH buffers. (C) pH dependence of VA oxidation by LiP*. Reaction mixtures contained 10 mM VA, 0.1 mM $H_2O_2$, and 40 nM LiP* in 20 mM sodium succinate buffer at given pH (reactions were initiated by addition of $H_2O_2$). Activities were estimated from maximum slope of absorbance changes at 310 nm, and relative values are shown.

at 37 °C and, completely inactivated after 30 min at 60 °C (Fig. 5A). Concerning pH, the LiP* was stable from 3.5 to neutral pH, but unstable over pH 7.0 and below pH 3.0 (Fig. 5B). The above stability properties were similar to those found for the wild enzyme. The pH dependence on VA oxidation by LiP* was also investigated (Fig. 5C). The recombinant peroxidase showed the highest activity at the lowest pH (~2.5), as previously found for wild *T. cervina* LiP [23]. Acidic pH is considered to increase the oxidation power of heme, enabling LiP and VP to oxidize VA [33].

Conservation of the catalytic properties of the wild LiP from *T. cervina*, namely its high oxidative potential and ability to oxidize large substrates [23], was confirmed by the results obtained with 1,4-dimethoxybenzene and ferrocytochrome *c*. Fig. 6A shows the spectral changes during 1,4-dimethoxybenzene oxidation by the recombinant enzyme. The 1,4-dimethoxybenzene peak at 286 nm gradually decreased, and a new peak at 254 nm appeared, suggesting that LiP* oxidized 1,4-dimethoxybenzene to 1,4-benzoquinone. On the other hand, Fig. 6B shows ferrocytochrome *c* oxidation by *T. cervina* LiP*. The ferrocytochrome *c* spectrum with peaks at 550 and 520 nm was converted into a new spectrum with a peak at 528 nm, revealing the formation of ferricytochrome *c*. These results indicated that LiP* possesses catalytic properties similar to those of wild LiP from *T. cervina*.

### *VA oxidation by T. cervina LiP**

Fig. 7A shows the absorbance changes at 310 nm (corresponding to the characteristic veratraldehyde maximum) during VA oxidation by LiP*. The trace showed an unexpected initial lag (around 20 s) in veratraldehyde formation. The lag was also observed when

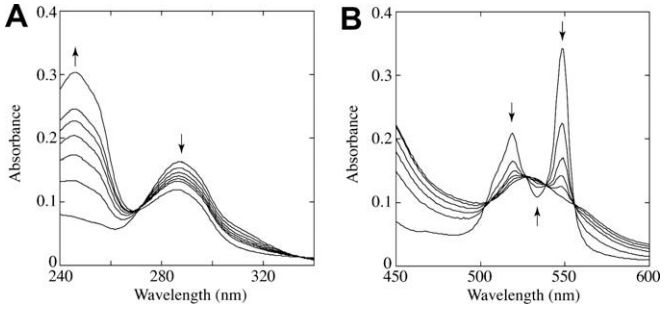


**Fig. 6.** Spectrophotometric demonstration of LiP* oxidation of 1,4-dimethoxybenzene (A) and ferrocytochrome *c* (B). The first scan was recorded before addition of $H_2O_2$, and the subsequent scans were recorded every 10 min in (A) and every minute in (B) after $H_2O_2$ addition. Arrows indicate the sense of the spectral changes.

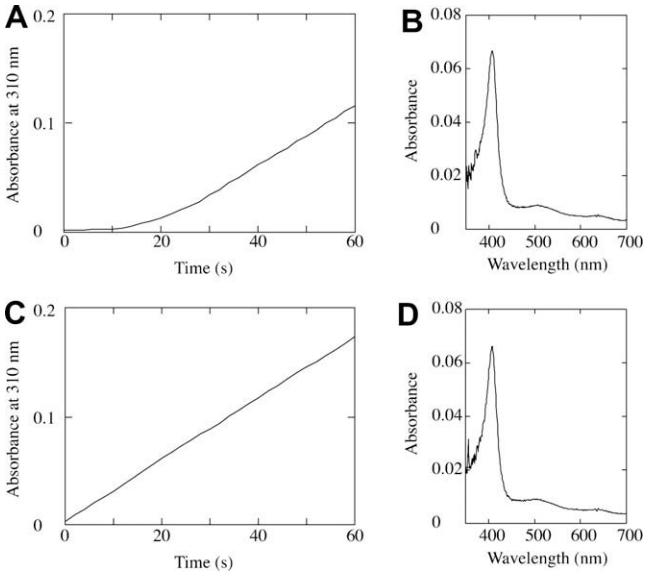


**Fig. 7.** Comparison of LiP* before and after pretreatment with VA and $H_2O_2$. Absorbance changes at 310 nm during VA oxidation by LiP* (A) showed an initial lag period in veratraldehyde formation that disappeared when the pretreated enzyme (p-LiP*) was used (C). The reaction mixture contained 10 mM VA, 0.1 mM $H_2O_2$, and 90 nM enzyme, in 20 mM sodium succinate buffer (pH 3.5). Absorption spectra of ~0.5 μM LiP* (B) and p-LiP* (D) in 20 mM sodium succinate buffer (pH 4.5), containing 1 mM $CaCl_2$, are also shown.

distilled VA was used as substrate, indicating that it was not due to the presence of a VA minor contaminant yielding an oxidation product with a different absorbance maximum. Therefore, it was considered that the *T. cervina* LiP* could undergo an autoxidative modification at the beginning of the reaction, resulting in enzyme activation.

The above hypothesis was supported by the fact that pretreated LiP* (p-LiP*) prepared by pre-incubating the recombinant enzyme with VA and $H_2O_2$ followed by dialysis (see Materials and methods) did not show any lag in veratraldehyde formation (Fig. 7C). The absorption spectrum of p-LiP* was identical to that of LiP* (Fig. 7B and D) indicating that the self-activation reaction does not affect the heme environment, but could affect the catalytic Tyr181 or its environment.

The VA oxidation activity of p-LiP* was almost identical to that of the *T. cervina* LiP* after the initial lag. In Table 2, the steady-state kinetic constants for VA oxidation by *E. coli*-expressed LiP*, before and after the above pretreatment, and wild LiP from *T. cervina* cul-

**Table 2**
Steady-state kinetics parameters for VA oxidation by pristine LiP* and after its VA–$H_2O_2$ pretreatment (p-LiP*) compared with wild LiP from *T. cervina* culture.

| | $K_m$ (μM) | $k_{cat}$ ($s^{-1}$) | $k_{cat}/K_m$ ($mM^{-1}\,s^{-1}$) |
|---|---|---|---|
| LiP* | 2790 | 16.3 | 5.8 |
| P-LiP* | 3240 | 17.7 | 5.5 |
| Wild *T. cervina* LiP[a] | 369 | 19.3 | 52.3 |

Reactions were performed in 20 mM sodium succinate buffer (pH 3.0) containing 0.1 mM $H_2O_2$, and 50 nM enzyme.
[a] The constants of wild *T. cervina* LiP are from [23].

ture are summarized. The constants showed no significant differences between LiP* and p-LiP*. When comparing to wild LiP, the $k_{cat}$ values were comparable (16–19 $s^{-1}$) but the $K_m$ values of the recombinant enzymes (LiP* and p-LiP*, ~3 mM) were approximately 8-fold higher than that of the wild enzyme (~0.4 mM), most probably because of the lack of glycosylation in the recombinant enzyme.

## Concluding comments

In this study, an *E. coli* expression system was constructed for the unique LiP from *T. cervina*, which has been reported to have a catalytic tyrosine residue [27]. *In vitro* refolding was optimized yielding a recombinant LiP* whose catalytic properties were the same of the wild LiP from *T. cervina* culture. Additionally, it was found that pristine LiP* from *E. coli* culture, which has never been in contact with its oxidizing/reducing substrates, presented an initial lag period in VA oxidation assays. The hypothesis that this could correspond to an initial self-activation of the enzyme is supported by the fact that p-LiP*, obtained after several turnovers in the presence of VA and $H_2O_2$, did not show the above lag. Although no significant difference between LiP* and p-LiP*, except for the lag in VA oxidation, was observed in the present study, p-LiP* may contain some structural modification, as reported in *P. chrysosporium* LiP and other peroxidases that experience autocatalytic modifications [15,34,35]. In the wild enzyme, this modification may occur naturally in the extracellular medium, which would contain VA (or other non-phenolic aromatic substrates) and $H_2O_2$ *de novo* synthesized by fungus [36,37]. The detailed structural and functional features of p-LiP* are of interest, and the corresponding analyses are in progress. Moreover, the heterologous expression system optimized here will permit to investigate structure–function relationships in the unique *T. cervina* LiP by site-directed mutagenesis and other techniques.

## Acknowledgments

This work was supported by the Spanish Projects BIO2007-65890-C02-01 and BIO2008-01533, and the BIORENEW project of the European Union (Contract NMP2-CT-2006-026456). Y.M. and F.J.R.-D. acknowledge two EU project contracts, and M.M. acknowledges a FPI fellowship of the Spanish MICINN.

## References

[1] G. Gellerstedt, G. Henriksson, Lignins: major sources, structure and properties, in: M. Belgacem, A. Gandini (Eds.), Monomers, Polymers and Composites from Renewable Resources, Elsevier, Amsterdam, 2008, pp. 201–224.
[2] W.G. Glasser, R.A. Northey, T.P. Schultz, Lignin: Historical, Biological, and Materials Perspectives, American Chemical Society, 2000.
[3] M. Tien, T.K. Kirk, Lignin-degrading enzyme from the hymenomycete *Phanerochaete chrysosporium* Burds, Science 221 (1983) 661–663.
[4] J.K. Glenn, M.A. Morgan, M.B. Mayfield, M. Kuwahara, M.H. Gold, An extracellular $H_2O_2$-requiring enzyme preparation involved in lignin biodegradation by the white rot basidiomycete *Phanerochaete chrysosporium*, Biochem. Biophys. Res. Commun. 114 (1983) 1077–1083.
[5] M. Tien, T.K. Kirk, Lignin-degrading enzyme from *Phanerochaete chrysosporium*: purification, characterization, and catalytic properties of a unique $H_2O_2$-requiring oxygenase, Proc. Natl. Acad. Sci. USA 81 (1984) 2280–2284.
[6] K.E. Hammel, D. Cullen, Role of fungal peroxidases in biological ligninolysis, Curr. Opin. Plant Biol. 11 (2008) 349–355.
[7] F.J. Ruiz-Dueñas, A.T. Martínez, Microbial degradation of lignin: how a bulky recalcitrant polymer is efficiently recycled in nature and how we can take advantage of this, Microb. Biotechnol. 2 (2009) 164–177.
[8] P.J. Kersten, B. Kalyanaraman, K.E. Hammel, B. Reinhammar, T.K. Kirk, Comparison of lignin peroxidase, horseradish peroxidase and laccase in the oxidation of methoxybenzenes, Biochem. J. 268 (1990) 475–480.
[9] H. Wariishi, D.W. Sheng, M.H. Gold, Oxidation of ferrocytochrome *c* by lignin peroxidase, Biochemistry 33 (1994) 5545–5552.
[10] T.K. Kirk, R.L. Farrell, Enzymatic "combustion": the microbial degradation of lignin, Annu. Rev. Microbiol. 41 (1987) 465–505.
[11] K.E. Hammel, K.A. Jensen, M.D. Mozuch, L.L. Landucci, M. Tien, E.A. Pease, Ligninolysis by a purified lignin peroxidase, J. Biol. Chem. 268 (1993) 12274–12281.
[12] A.T. Martínez, F.J. Ruiz-Dueñas, M.J. Martínez, J.C. del Río, A. Gutiérrez, Enzymatic delignification of plant cell-wall: from nature to mill, Curr. Opin. Biotechnol. (2009), doi: 10.1016/j.copbio.2009.05.002.
[13] T. Mester, K. Ambert-Balay, S. Ciofi-Baffoni, L. Banci, A.D. Jones, M. Tien, Oxidation of a tetrameric nonphenolic lignin model compound by lignin peroxidase, J. Biol. Chem. 276 (2001) 22985–22990.
[14] W.A. Doyle, W. Blodig, N.C. Veitch, K. Piontek, A.T. Smith, Two substrate interaction sites in lignin peroxidase revealed by site-directed mutagenesis, Biochemistry 37 (1998) 15097–15105.
[15] W. Blodig, A.T. Smith, W.A. Doyle, K. Piontek, Crystal structures of pristine and oxidatively processed lignin peroxidase expressed in *Escherichia coli* and of the W171F variant that eliminates the redox active tryptophan 171. Implications for the reaction mechanism, J. Mol. Biol. 305 (2001) 851–861.
[16] M.D.S. Gelpke, J. Lee, M.H. Gold, Lignin peroxidase oxidation of veratryl alcohol: effects of the mutants H82A, Q222A, W171A, and F267L, Biochemistry 41 (2002) 3498–3506.
[17] T. Johjima, H. Wariishi, H. Tanaka, Veratryl alcohol binding sites of lignin peroxidase from *Phanerochaete chrysosporium*, J. Mol. Catal. B: Enzym. 17 (2002) 49–57.
[18] M. Pérez-Boada, F.J. Ruiz-Dueñas, R. Pogni, R. Basosi, T. Choinowski, M.J. Martínez, K. Piontek, A.T. Martínez, Versatile peroxidase oxidation of high redox potential aromatic compounds: site-directed mutagenesis, spectroscopic and crystallographic investigations of three long-range electron transfer pathways, J. Mol. Biol. 354 (2005) 385–402.
[19] F.J. Ruiz-Dueñas, M. Morales, M.J. Mate, A. Romero, M.J. Martínez, A.T. Smith, A.T. Martínez, Site-directed mutagenesis of the catalytic tryptophan environment in *Pleurotus eryngii* versatile peroxidase, Biochemistry 47 (2008) 1685–1695.
[20] T. Tsukihara, Y. Honda, R. Sakai, T. Watanabe, T. Watanabe, Mechanism for oxidation of high-molecular-weight substrates by a fungal versatile peroxidase, MnP2, Appl. Environ. Microbiol. 74 (2008) 2873–2881.
[21] A.T. Martínez, Molecular biology and structure–function of lignin-degrading heme peroxidases, Enzyme Microb. Technol. 30 (2002) 425–444.
[22] F.J. Ruiz-Dueñas, M. Morales, E. García, Y. Miki, M.J. Martínez, A.T. Martínez, Substrate oxidation sites in versatile peroxidase and other basidiomycete peroxidases, J. Exp. Bot. 60 (2009) 441–452.
[23] Y. Miki, H. Tanaka, M. Nakamura, H. Wariishi, Isolation and characterization of a novel lignin peroxidase from the white-rot basidiomycete *Trametes cervina*, J. Fac. Agr. Kyushu Univ. 51 (2006) 99–104.
[24] Y. Miki, H. Wariishi, H. Tanaka, Lignin peroxidase from the white-rot basidiomycete *Trametes cervina*, in: Proceedings of the 12th ISWPC, vol. II, Madison, 9–12 June, 2003, p. 95.
[25] J. Stubbe, W.A. Der Donk, Protein radicals in enzyme catalysis, Chem. Rev. 98 (1998) 705–762.
[26] F.J. Ruiz-Dueñas, R. Pogni, M. Morales, S. Giansanti, M.J. Mate, A. Romero, M.J. Martínez, R. Basosi, A.T. Martínez, Protein radicals in fungal versatile peroxidase: catalytic tryptophan radical in both compound I and compound II and studies on W164Y, W164H and W164S variants, J. Biol. Chem. 284 (2009) 7986–7994.
[27] Y. Miki, H. Wariishi, Molecular characterization of a novel lignin peroxidase from the white-rot basidiomycete *Trametes cervina*, in: Proceedings of the International Symposium on Mushroom Science, Akita, Japan, 20–22 September, 2006, pp. 183–184.
[28] A.T. Smith, N. Santama, S. Dacey, M. Edwards, R.C. Bray, R.N.F. Thorneley, J.F. Burke, Expression of a synthetic gene for horseradish peroxidase C in *Escherichia coli* and folding and activation of the recombinant enzyme with $Ca^{2+}$ and heme, J. Biol. Chem. 265 (1990) 13335–13343.
[29] R. Whitwam, M. Tien, Heterologous expression and reconstitution of fungal Mn peroxidase, Arch. Biochem. Biophys. 333 (1996) 439–446.
[30] W.A. Doyle, A.T. Smith, Expression of lignin peroxidase H8 in *Escherichia coli*: folding and activation of the recombinant enzyme with $Ca^{2+}$ and haem, Biochem. J. 315 (1996) 15–19.
[31] M. Pérez-Boada, W.A. Doyle, F.J. Ruiz-Dueñas, M.J. Martínez, A.T. Martínez, A.T. Smith, Expression of *Pleurotus eryngii* versatile peroxidase in *Escherichia coli* and optimisation of in vitro folding, Enzyme Microb. Technol. 30 (2002) 518–524.

[32] M.M. Bradford, A rapid and sensitive method for the quantitation of microgram quantities of proteins utilizing the principle of protein-dye binding, Anal. Biochem. 72 (1976) 248–254.
[33] M. Oyadomari, H. Shinohara, T. Johjima, H. Wariishi, H. Tanaka, Electrochemical characterization of lignin peroxidase from the white-rot basidiomycete *Phanerochaete chrysosporium*, J. Mol. Catal. B: Enzym. 21 (2003) 291–297.
[34] J. Zeng, R.E. Fenna, X-ray crystal structure of canine myeloperoxidase at 3 Å resolution, J. Mol. Biol. 226 (2009) 185–207.
[35] X. Carpena, S. Loprasert, S. Mongkolsuk, J. Switala, P.C. Loewen, I. Fita, Catalase-peroxidase KatG of *Burkholderia pseudomallei* at 1.7 Å resolution, J. Mol. Biol. 327 (2009) 475–489.
[36] M. Shimada, F. Nakatsubo, T.K. Kirk, T. Higuchi, Biosynthesis of the secondary metabolite veratryl alcohol in relation to lignin degradation by *Phanerochaete chrysosporium*, Arch. Microbiol. 129 (1981) 321–324.
[37] P.J. Kersten, T.K. Kirk, Involvement of a new enzyme, glyoxal oxidase, in extracellular $H_2O_2$ production by *Phanerochaete chrysosporium*, J. Bacteriol. 169 (1987) 2195–2201.